Human LilrB2 Is a β-Amyloid Receptor and Its Murine Homolog PirB Regulates Synaptic Plasticity in an Alzheimer's Model

Taeho Kim *et al.*

Science **341**, 1399 (2013);
DOI: 10.1126/science.1242077

Science (print ISSN 0036-8075; online ISSN 1095-9203) is published weekly, except the last week in December, by the American Association for the Advancement of Science, 1200 New York Avenue NW, Washington, DC 20005.

11. S. B. Lane-Ladd *et al.*, *J. Neurosci.* **17**, 7890–7901 (1997).
12. R. Drdla, M. Gassner, E. Gingl, J. Sandkühler, *Science* **325**, 207–210 (2009).
13. C. Heinl, R. Drdla-Schutting, D. N. Xanthos, J. Sandkühler, *J. Neurosci.* **31**, 16748–16756 (2011).
14. E. J. Nestler, G. K. Aghajanian, *Science* **278**, 58–63 (1997).
15. J. A. Kauer, R. C. Malenka, *Nat. Rev. Neurosci.* **8**, 844–858 (2007).
16. M. S. Angst, J. D. Clark, *Anesthesiology* **104**, 570–587 (2006).
17. Z. Wang, E. J. Bilsky, F. Porreca, W. Sadée, *Life Sci.* **54**, PL339–PL350 (1994).
18. J. G. Liu, P. L. Prather, *Mol. Pharmacol.* **60**, 53–62 (2001).
19. D. Wang *et al.*, *J. Pharmacol. Exp. Ther.* **308**, 512–520 (2004).
20. J. R. Shoblock, N. T. Maidment, *Neuropsychopharmacology* **31**, 171–177 (2006).
21. F. J. Meye, R. van Zessen, M. P. Smidt, R. A. Adan, G. M. Ramakers, *J. Neurosci.* **32**, 16120–16128 (2012).
22. J. R. Shoblock, N. T. Maidment, *Neuroscience* **149**, 642–649 (2007).
23. E. M. Pogatzki, S. N. Raja, *Anesthesiology* **99**, 1023–1027 (2003).
24. C. Luo, P. H. Seeburg, R. Sprengel, R. Kuner, *Pain* **140**, 358–367 (2008).
25. S. Doolen, C. B. Blake, B. N. Smith, B. K. Taylor, *Mol. Pain* **8**, 56 (2012).
26. D. M. Chetkovich, J. D. Sweatt, *J. Neurochem.* **61**, 1933–1942 (1993).
27. V. Zachariou *et al.*, *Biol. Psychiatry* **63**, 1013–1021 (2008).
28. M. S. Mazei-Robison, E. J. Nestler, *Cold Spring Harbor Perspect. Med.* **2**, a012070 (2012).
29. F. Wei *et al.*, *Neuron* **36**, 713–726 (2002).
30. H. Wang *et al.*, *Sci. Transl. Med.* **3**, 65ra3 (2011).
31. T. Kenakin, *FASEB J.* **15**, 598–611 (2001).
32. T. Kenakin, *Trends Pharmacol. Sci.* **25**, 186–192 (2004).
33. T. Costa, A. Herz, *Proc. Natl. Acad. Sci. U.S.A.* **86**, 7321–7325 (1989).
34. R. Seifert, K. Wenzel-Seifert, *Naunyn Schmiedebergs Arch. Pharmacol.* **366**, 381–416 (2002).
35. K. M. Raehal *et al.*, *J. Pharmacol. Exp. Ther.* **313**, 1150–1162 (2005).
36. W. Sadée, D. Wang, E. J. Bilsky, *Life Sci.* **76**, 1427–1437 (2005).
37. H. Lam *et al.*, *Mol. Pain* **7**, 24 (2011).
38. J. G. Liu, M. B. Ruckle, P. L. Prather, *J. Biol. Chem.* **276**, 37779–37786 (2001).
39. T. King *et al.*, *Nat. Neurosci.* **12**, 1364–1366 (2009).
40. Y. He, X. Tian, X. Hu, F. Porreca, Z. J. Wang, *J. Pain* **13**, 598–607 (2012).
41. K. J. Sufka, *Pain* **58**, 355–366 (1994).
42. G. F. Koob, R. Maldonado, L. Stinus, *Trends Neurosci.* **15**, 186–191 (1992).
43. B. Kest *et al.*, *Neuroscience* **115**, 463–469 (2002).
44. M. N. Asiedu *et al.*, *J. Neurosci.* **31**, 6646–6653 (2011).
45. M. De Felice *et al.*, *Brain* **133**, 2475–2488 (2010).
46. C. Rivat *et al.*, *Neuropsychopharmacology* **32**, 2217–2228 (2007).
47. M. Zhuo, *Drug Discov. Today* **17**, 573–582 (2012).
48. S. Li *et al.*, *Mol. Pharmacol.* **70**, 1742–1749 (2006).
49. H. C. Lu *et al.*, *Nat. Neurosci.* **6**, 939–947 (2003).
50. H. Xu *et al.*, *J. Neurosci.* **28**, 7445–7453 (2008).
51. C. Rivat *et al.*, *Anesthesiology* **96**, 381–391 (2002).

Acknowledgments: The authors thank H. L. Fields, A. I. Basbaum, L. Hough, J. C. Marvizon, E. Bilsky, W. Sadee, G. Scherrer, K. Westlund High, M. Werner, J. Dahl, and B. Solway for critical discussions and J. Grasch, L. Martin, and R. Griggs for technical assistance and blinding. This work was supported by NIH grants F31DA032496 (G.C.), HD02528 (M.K.W. and K.E.M.), R01NS45954 (B.K.T.), and 5K02DA19656 (B.K.T.). Author contributions: G.C. and B.K.T. formulated the hypotheses, designed, analyzed and coordinated all experiments. G.C. performed surgeries, behavioral pharmacology, histology, and fluorescence imaging and analyzed the data. G.C. and B.L.J. carried out the biochemical studies and G.C. analyzed the data. S.D. and G.C. carried out Ca^{2+} imagining experiments and analyzed the data. M.K.W., K.E.M., G.C., and B.K.T. designed the [^{35}S]GTP-γ-S binding studies; M.K.W. collected the data; and G.C., K.E.M., and B.K.T. analyzed the data. D.R.S. supplied the AC1$^{-/-}$ breeders. Z.J.W., G.C., and B.K.T. designed the conditioned place preference experiments, and Y.H. and X.H. conducted experiments and analyzed the data. J.S.M., J.S.W., G.C., and B.K.T. designed the Mouse Grimace Scale experiments, and J.W. conducted the experiments. R.R.D. conducted the plantar incision studies. G.C. and B.K.T. wrote the manuscript.

Supplementary Materials

www.sciencemag.org/content/341/6152/1394/suppl/DC1
Materials and Methods
Supplementary Text
Figs. S1 to S13
References (*52*–*80*)

19 April 2013; accepted 20 August 2013
10.1126/science.1239403

Human LilrB2 Is a β-Amyloid Receptor and Its Murine Homolog PirB Regulates Synaptic Plasticity in an Alzheimer's Model

Taeho Kim,[1]* George S. Vidal,[1] Maja Djurisic,[1] Christopher M. William,[2] Michael E. Birnbaum,[3] K. Christopher Garcia,[3] Bradley T. Hyman,[2] Carla J. Shatz[1]*

Soluble β-amyloid (Aβ) oligomers impair synaptic plasticity and cause synaptic loss associated with Alzheimer's disease (AD). We report that murine PirB (paired immunoglobulin-like receptor B) and its human ortholog LilrB2 (leukocyte immunoglobulin-like receptor B2), present in human brain, are receptors for Aβ oligomers, with nanomolar affinity. The first two extracellular immunoglobulin (Ig) domains of PirB and LilrB2 mediate this interaction, leading to enhanced cofilin signaling, also seen in human AD brains. In mice, the deleterious effect of Aβ oligomers on hippocampal long-term potentiation required PirB, and in a transgenic model of AD, PirB not only contributed to memory deficits present in adult mice, but also mediated loss of synaptic plasticity in juvenile visual cortex. These findings imply that LilrB2 contributes to human AD neuropathology and suggest therapeutic uses of blocking LilrB2 function.

Soluble oligomeric species of β-amyloid (Aβ) are thought to be key mediators of cognitive dysfunction in Alzheimer's disease (AD) (*1*, *2*). Transgenic mice expressing elevated levels of human Aβ experience memory loss and synaptic regression (*3*–*6*). Aβ production is thought to be activity-dependent (*7*, *8*), and even in wild-type mice, addition of soluble Aβ oligomers to hippocampal slices or cultures induces loss of long-term potentiation (LTP), increases long-term depression (LTD), and decreases dendritic spine density (*9*–*11*). Aβ oligomers may exert some of their adverse effects on synaptic plasticity and memory by binding to receptors, thereby perturbing or engaging downstream signaling. At least two Aβ receptors, cellular prion protein (PrP^C) and ephrin type B receptor 2 (EphB2), have been identified, and downstream signaling from both alters *N*-methyl-D-aspartate (NMDA) receptor function in response to Aβ (*6*, *12*, *13*). Aβ oligomers are also known to engage other signaling pathways, including the actin-severing protein cofilin and protein phosphatases PP2A and PP2B/calcineurin, thereby mediating spine loss and synaptic defects (*9*, *14*); however, signaling upstream of these pathways is not well understood.

Recently, a very early loss of activity-dependent plasticity was discovered in vivo in APP/PS1 transgenic mice, an AD model in which mutant alleles of both amyloid precursor protein (APPswe) and presenilin 1 (PSEN1ΔE9) are expressed (*15*, *16*): Ocular dominance plasticity (ODP) during the critical period of development in visual cortex [postnatal day 22 (P22) to P32] is defective (*17*). This observation directly contrasts with mice lacking PirB (paired immunoglobulin-like receptor B), in which ODP is enhanced during the critical period and in adults (*18*). PirB, a receptor originally thought to function exclusively in the immune system (*19*), is now also known to be expressed by neurons, present in neuronal growth cones, and associated with synapses (*18*, *20*). Thus, it is possible that Aβ acts through PirB to diminish ODP in APP/PS1 mice.

To determine whether PirB can act as a receptor for soluble Aβ oligomers, we prepared biotinylated synthetic human $Aβ_{1-42}$ (Aβ42) peptides either without (mono-Aβ42) or with oligomerization (oligo-Aβ42; consists primarily of high-*n* oligomers) (Fig. 1, A and B, and fig. S1A) (*12*, *21*, *22*). We then measured binding of Aβ42 peptides to human embryonic kidney (HEK) 293 cells that expressed mouse PirB (PirB-IRES-EGFP) or control vector (IRES-EGFP). Relative to monomeric Aβ42, oligomerized Aβ42 peptides bound to PirB-expressing cells about 6 times as much (Fig. 1, A to D). Oligo-Aβ42 was consistently associated with PirB protein, as seen both by coimmunostaining (Fig. 1E, arrowheads) and by coimmunoprecipitation (fig. S1, B and C), indicating a direct interaction with PirB. This assay also confirms previously reported Nogo-66 binding to PirB (fig. S2) (*20*). In contrast, binding of Aβ42 oligomers was not evident in heterologous cells expressing mouse

[1]Departments of Biology and Neurobiology and Bio-X, James H. Clark Center, Stanford University, Stanford, CA 94305, USA. [2]Neuropathology Service, Massachusetts General Hospital, Charlestown, MA 02129, USA. [3]Howard Hughes Medical Institute, Department of Molecular and Cellular Physiology, and Department of Structural Biology, Stanford University School of Medicine, Stanford, CA 94305, USA.

*Corresponding author. E-mail: cshatz@stanford.edu (C.J.S.); tkim808@stanford.edu (T.K.)

PirA1, mouse PirA4, or an isoform of rat PirB (*23*); all of these receptors are closely related to mouse PirB (Fig. 1, F and G, and fig. S3). This finding indicates that Aβ42 oligomers bind selectively to PirB. Oligo-Aβ42 binding to PirB expressed in HEK293 cells was saturable, with an apparent dissociation constant (K_d) of 180 nM monomer equivalent of total Aβ42 peptide (Fig. 1, H to J) (*24*). An alkaline phosphatase assay gave a similar binding affinity (K_d = 160 nM; fig. S4). In contrast, mono-Aβ42 exhibited no apparent binding affinity to PirB (Fig. 1, H to J).

Aβ42 oligomer binding to cultured cortical neurons from PirB$^{-/-}$ mice was diminished by about 50% relative to wild-type neurons, indicating that binding is PirB-dependent. The estimated K_d for Aβ42 oligomers and neuronal PirB is 110 nM (Fig. 1K), similar to that observed for PirB-expressing HEK293 cells (Fig. 1, I and J). We note that this binding is not completely abolished in the absence of PirB (Fig. 1K), which suggests that additional binding sites for Aβ oligomers exist (*6*, *12*, *25*). Together, these results suggest that PirB is a high-affinity receptor for Aβ oligomers.

The human homolog of murine PirB is leukocyte immunoglobulin (Ig)–like receptor B, which comprises five family members, LilrB1 to LilrB5 (*19*, *20*). To identify which of these orthologs functions analogously to PirB as a receptor for Aβ oligomers, we examined the three most related LilrB receptors, LilrB1, 2, and 3 (*19*, *20*, *26*, *27*), as well as a moderately related human killer immune receptor (Kir) (Fig. 2A). Aβ42 oligomers robustly bound to LilrB2-expressing heterologous cells, but not to LilrB1-, LilrB3-, or Kir (3DL1)–expressing cells (Fig. 2B and fig. S5A). Binding was saturable, with an apparent K_d of 206 nM (Fig. 2, C and D; also fig. S5, B and C: K_d = 250 nM). LilrB2 displayed minimal binding to mono-Aβ42 (Fig. 2, C and D), which suggests selective binding with Aβ42 oligomers. LilrB2 proteins were detected in human brain specimens from

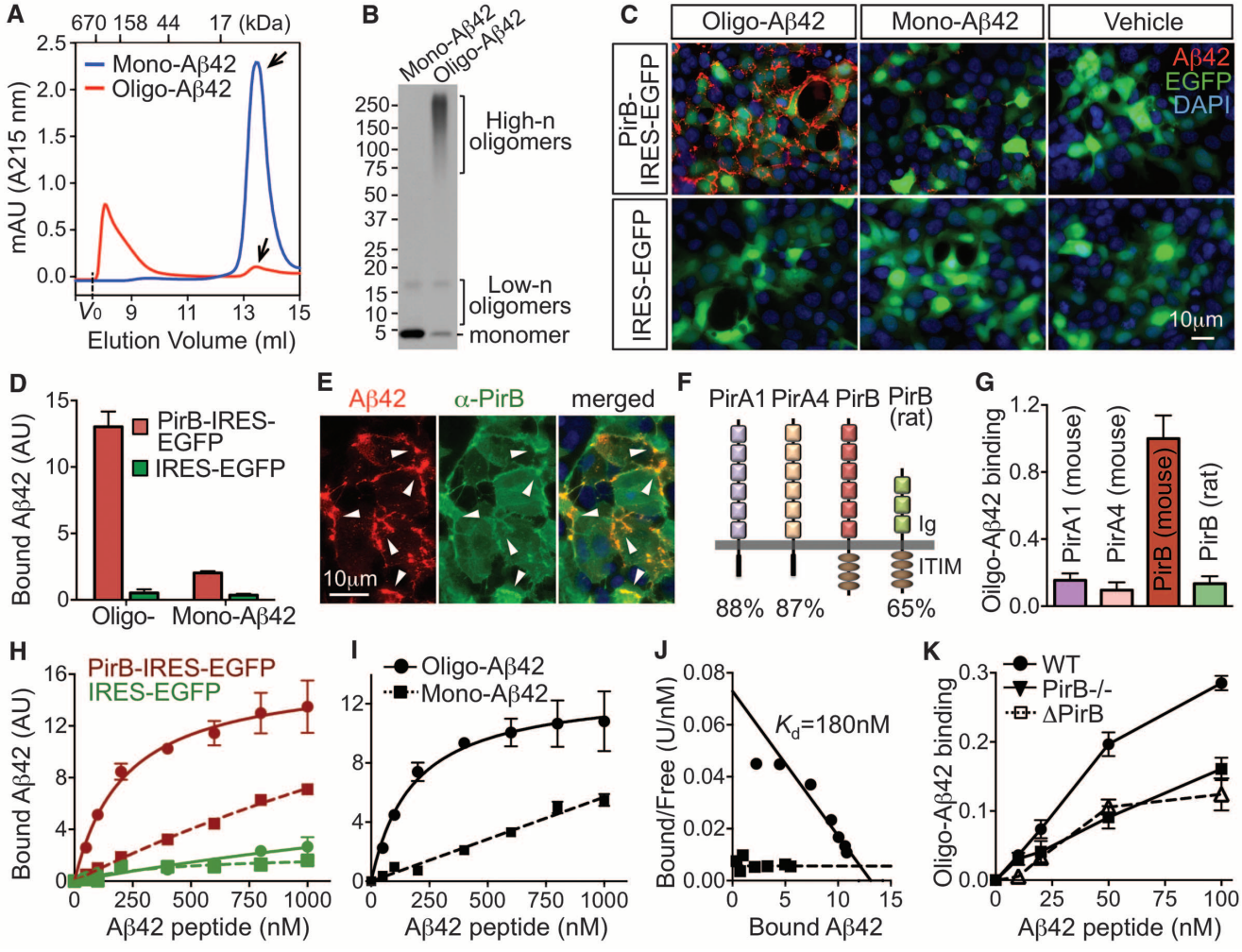

Fig. 1. PirB is a receptor for oligomeric Aβ. (**A**) Monomeric (mono) or oligomerized (oligo) synthetic human Aβ42 peptides (fig. S1A) (*21*, *22*) were analyzed by size exclusion column chromatography. Arrows indicate monomeric form; V_0, void volume; absorbance at 215 nm is in arbitrary units. (**B**) The same peptides were analyzed by Western blotting with antibody to Aβ (4G8; detects Aβ17-24). (**C**) PirB-IRES-EGFP–transfected (top) or control IRES-EGFP–transfected (bottom) HEK293 cells (green) were treated with mono- or oligo-Aβ42 (100 nM total peptide, monomer equivalent), and bound Aβ42 (red) was visualized. See also fig. S1. DAPI, 4′,6-diamidino-2-phenylindole. (**D**) Quantification of Aβ42 binding represented in (C). AU denotes average signal per pixel (*22*); data are means ± SEM (PirB-IRES-EGFP, n = 5; IRES-EGFP, n = 4). (**E**) PirB-expressing cells were treated with oligo-Aβ42 (100 nM) and immunostained for Aβ and PirB. Colocalization is observed particularly at cell membrane (i.e., arrowheads). (**F**) Schematic of mouse PirB, the highly related mouse PirA1 and PirA4, and a rat PirB isoform (*23*). Amino acid sequence similarities to mouse PirB (% score, ClustalW) are indicated at bottom. Ig, immunoglobulin domain; ITIM, immunoreceptor tyrosine-based inhibitory motif. (**G**) Relative oligo-Aβ42 (200 nM) binding to HEK293 cells expressing mouse PirB, PirA1, or PirA4 or rat PirB; see also fig. S3. Data are means ± SEM (n = 4 or 5). (**H**) Dose-dependent binding of mono- or oligo-Aβ42 (squares and circles, respectively) to HEK293 cells expressing IRES-EGFP (green) or PirB-IRES-EGFP (red), assessed as a function of Aβ42 total concentration. (**I**) Binding curve of mono- or oligo-Aβ42 to PirB. Data (PirB-IRES-EGFP minus IRES-EGFP) are from (H) (*22*). (**J**) Scatchard plots of data from (I). Data are means ± SEM (n = 4). Calculated K_d = 180 ± 52 nM; see also fig. S4. (**K**) Binding of oligo-Aβ42 to cultured cortical neurons (21 days in vitro) is diminished ~50% by deletion of PirB (PirB$^{-/-}$), as assessed by alkaline phosphatase assay. Data are means ± SEM (n = 6). Estimated K_d for neuronal PirB [dashed line: ΔPirB = wild type (WT) minus PirB$^{-/-}$] is 110 nM.

both AD patients and non-AD adults (table S1), with no significant difference in levels (Fig. 2, E and F); however, downstream signaling was altered in AD (see below). These results suggest that LilrB2 is available as a receptor for Aβ oligomers in human brain. LilrB2 has also been identified as a human ortholog of PirB for other recently discovered nonimmune ligands: In vitro, PirB and LilrB2 act as functional receptors to inhibit axonal outgrowth on Nogo, myelin-associated glycoprotein, and oligodendrocyte myelin glycoprotein substrates (*20*); in the hematopoetic system, angiopoietin-like proteins can also bind to PirB and LilrB2 to support stem cell and leukemia development (*26*). These observations imply that mouse PirB may have diverse functions well beyond inhibitory signaling in the innate immune system and that LilrB2 may execute these roles in humans, particularly in the nervous system.

To determine the domains of PirB or LilrB2 responsible for Aβ oligomer binding, we made full-length or deletion mutants of PirB and LilrB2 (Fig. 2G). Because Aβ oligomers appear to bind preferentially to dimeric PirB in heterologous cells (fig. S6A), soluble dimeric forms of PirB or LilrB2 extracellular domain were constructed using human IgG1-Fc (fig. S6B). In vitro binding to Aβ42 oligomers revealed that the two most N-terminal Ig domains (D1D2) of PirB and of LilrB2 are critical, whereas the PirB-D5D6 and LilrB2-D3D4 domains have minimal affinity (Fig. 2, G and H, and fig. S6C) (*28*). In this assay, PirB-Fc, LilrB2-Fc, and PirB(D1D2)-Fc proteins pulled down high-*n* Aβ42 oligomers (Fig. 2H), recapitulating coimmunoprecipitation results (fig. S1B). PirB(D5D6)-Fc was used as a negative control and the oligomeric status of bound Aβ42 was confirmed using the oligomer-specific antibody OMAB (*29*) (Fig. 2H and fig. S6D). These results suggest that PirB and LilrB2 are potent receptors for Aβ42 oligomers, and that their D1D2 domains are sufficient to mediate binding.

If PirB or LilrB2 mediates deleterious effects of Aβ on synaptic function, then deletion of PirB should mitigate them in cellular or animal models of AD. A cellular mechanism proposed to underlie memory impairment in AD is loss of hippocampal LTP resulting from the presence of soluble Aβ oligomers (*2*, *12*). To assess a direct contribution of PirB to this cellular correlate of AD pathology, we examined the effects of acute Aβ42 oligomer addition in wild-type and PirB$^{-/-}$ hippocampal slices; LTP at Schaffer collateral-CA1 synapses was measured (Fig. 3, A to D). Because PirB has high affinity for Aβ oligomers ($K_d \approx 110$ to 180 nM; Fig. 1 and fig. S4), slices were treated with 200 nM total peptide of oligomerized Aβ42 or with vehicle control, and field

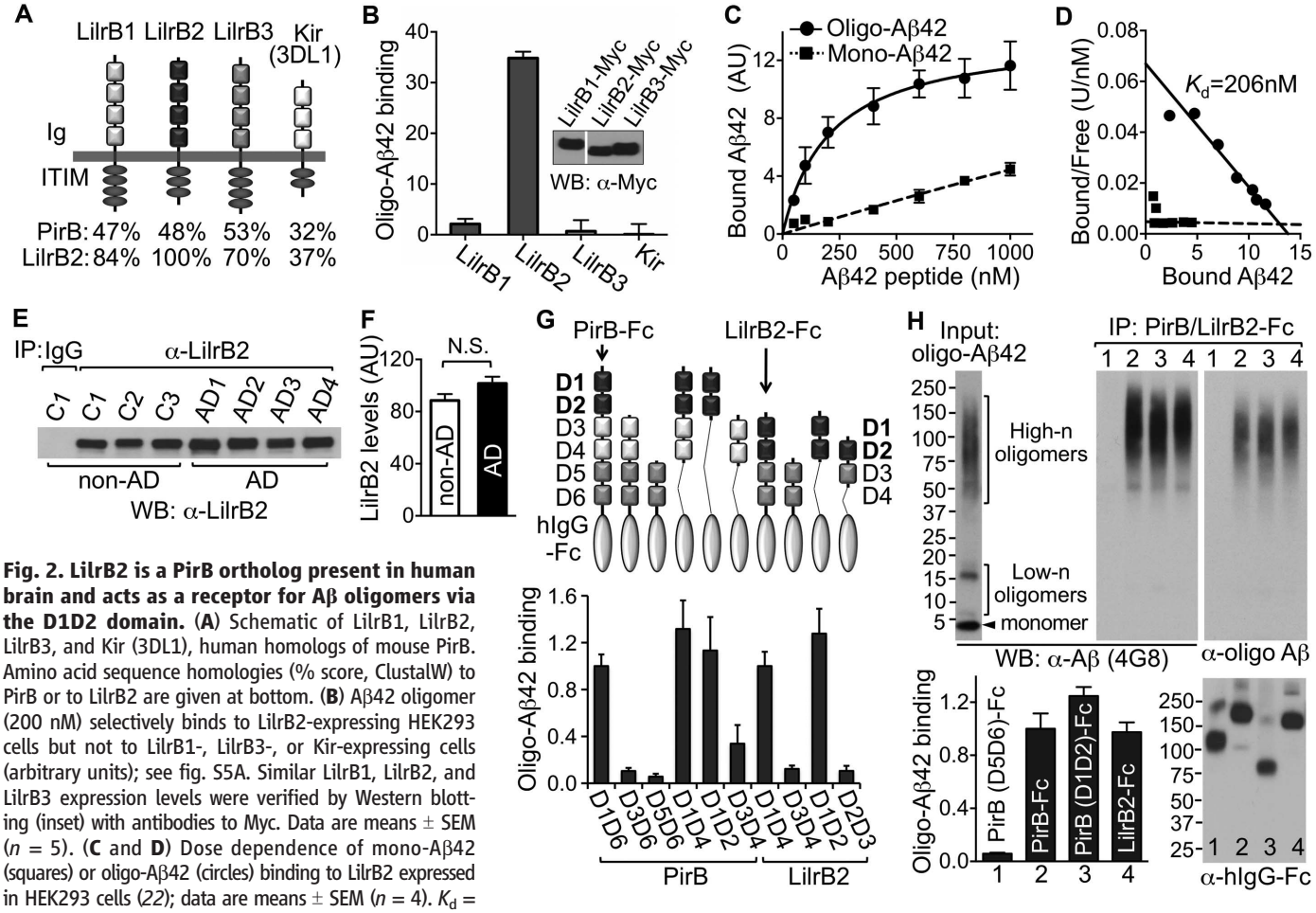

Fig. 2. LilrB2 is a PirB ortholog present in human brain and acts as a receptor for Aβ oligomers via the D1D2 domain. (**A**) Schematic of LilrB1, LilrB2, LilrB3, and Kir (3DL1), human homologs of mouse PirB. Amino acid sequence homologies (% score, ClustalW) to PirB or to LilrB2 are given at bottom. (**B**) Aβ42 oligomer (200 nM) selectively binds to LilrB2-expressing HEK293 cells but not to LilrB1-, LilrB3-, or Kir-expressing cells (arbitrary units); see fig. S5A. Similar LilrB1, LilrB2, and LilrB3 expression levels were verified by Western blotting (inset) with antibodies to Myc. Data are means ± SEM (n = 5). (**C** and **D**) Dose dependence of mono-Aβ42 (squares) or oligo-Aβ42 (circles) binding to LilrB2 expressed in HEK293 cells (*22*); data are means ± SEM (n = 4). K_d = 206 ± 65 nM; see also fig. S5, B and C. (**E**) LilrB2 is expressed in frontal lobe of specimens from three adult humans (non-AD; C1 to C3) and from four Alzheimer's patients (AD1 to AD4) (table S1). Protein extracts from fresh frozen frontal lobe were immunoprecipitated with control IgG or LilrB2-specific antibodies followed by Western blot analysis. (**F**) Quantitation of LilrB2 protein levels shown in (E). Data are means ± SEM. (**G**) Deletion of the D1D2 domain abrogates binding of Aβ42 oligomers to PirB and LilrB2. Top: Schematic of PirB and LilrB2 ectodomain constructs: full-length or truncated Ig domains fused to human IgG-Fc (hIgG-Fc). Bottom: Bar graphs of average band intensities ± SEM from experiments such as that shown in fig. S6C (n = 3). Note that sequence analysis using pairwise alignment indicates that the D1D2 domain of LilrB2 aligns closely with the D1D2 domain of PirB (*28*). (**H**) PirB-Fc or LilrB2-Fc binds predominantly to high-*n* oligomeric forms of Aβ42. Oligomerized Aβ42 (input; also contains low-*n* oligomers and monomeric Aβ42) was subjected to immunoprecipitation with full-length or truncated soluble PirB- or LilrB2-Fc proteins followed by Western blot analysis. Aβ oligomer binding domain–deficient PirB (D5D6)-Fc treatment was used as negative control (lane 1). Top right: Western blot with antibodies to Aβ specific for oligomeric forms (OMAB; see fig. S6D); Bottom left: quantification of Aβ42 binding. Data are normalized average band intensities ± SEM (n = 3).

excitatory postsynaptic potentials (fEPSPs) after theta burst stimulation (TBS) were recorded. Consistent with previous reports (*12*, *30*), Aβ42 oligomers abolished LTP in hippocampal slices from wild-type mice (vehicle, 134 ± 4% of baseline; Aβ42 oligomer, 94 ± 7% of baseline; Fig. 3, A and C). In marked contrast, in PirB$^{-/-}$ slices, LTP remained intact even in the presence of Aβ42 oligomers (135 ± 5% of baseline; Fig. 3, B and C); these effects were significantly different between wild-type and PirB$^{-/-}$ slices (Fig. 3D). Application of vehicle control in PirB$^{-/-}$ slices did not alter the magnitude of LTP, which was similar to wild-type mice (125 ± 4% of baseline; Fig. 3, B and C), consistent with previous observations of hippocampal LTP in PirB$^{-/-}$ mice (*31*). These experiments demonstrate that the deleterious effects of Aβ oligomers on hippocampal LTP depend on PirB.

To assess whether PirB contributes in vivo to cognitive deficits, we crossed APP/PS1 transgenic (Tg) mice with PirB$^{-/-}$ mice to generate APP/PS1 littermates with (PirB$^{+/-}$ Tg) or without (PirB$^{-/-}$ Tg) PirB. First, recognition memory was examined using two tests: novel object recognition and novel place recognition (*6*, *32*). As expected (*32*), impaired behaviors were observed in both tests in 9-month-old PirB$^{+/-}$ Tg mice; however, these learning and memory defects were not evident in mice lacking PirB (PirB$^{-/-}$ Tg) (Fig. 3, E and F). Together, these observations demonstrate that PirB contributes not only to Aβ-mediated loss of hippocampal LTP but also to defects in recognition memory that characterize older APP/PS1 mice and are symptoms of synaptic pathology in AD.

One of the earliest manifestations of pathology detected in APP/PS1 mice is impaired ODP (*17*). We evaluated ODP during the developmental critical period (P22 to P32) by measuring the ability of one eye to expand its functional representation within visual cortex after removal of the other eye (Fig. 3G). ODP was significantly diminished in APP/PS1 mice (PirB$^{+/-}$ Tg) (18%; Fig. 3, H and I) (*17*). When we deleted PirB, the mice (PirB$^{-/-}$ Tg) showed no loss in ODP. In fact, PirB$^{-/-}$ Tg mice had ODP similar to that of PirB$^{-/-}$ mice and greater than that of PirB$^{+/-}$ mice (Fig. 3, H and I), consistent with previous observations (*18*) and with the fact that PirB binds other ligands known to limit ODP in addition to Aβ (i.e., MHCI; Nogo; fig. S2 and S10) (*18*, *20*, *33*).

Cellular mechanisms associated with ODP in visual cortex of juvenile APP/PS1 mice were also examined. LTD of synaptic responses in cortical layer 2/3 induced by low-frequency stimulation

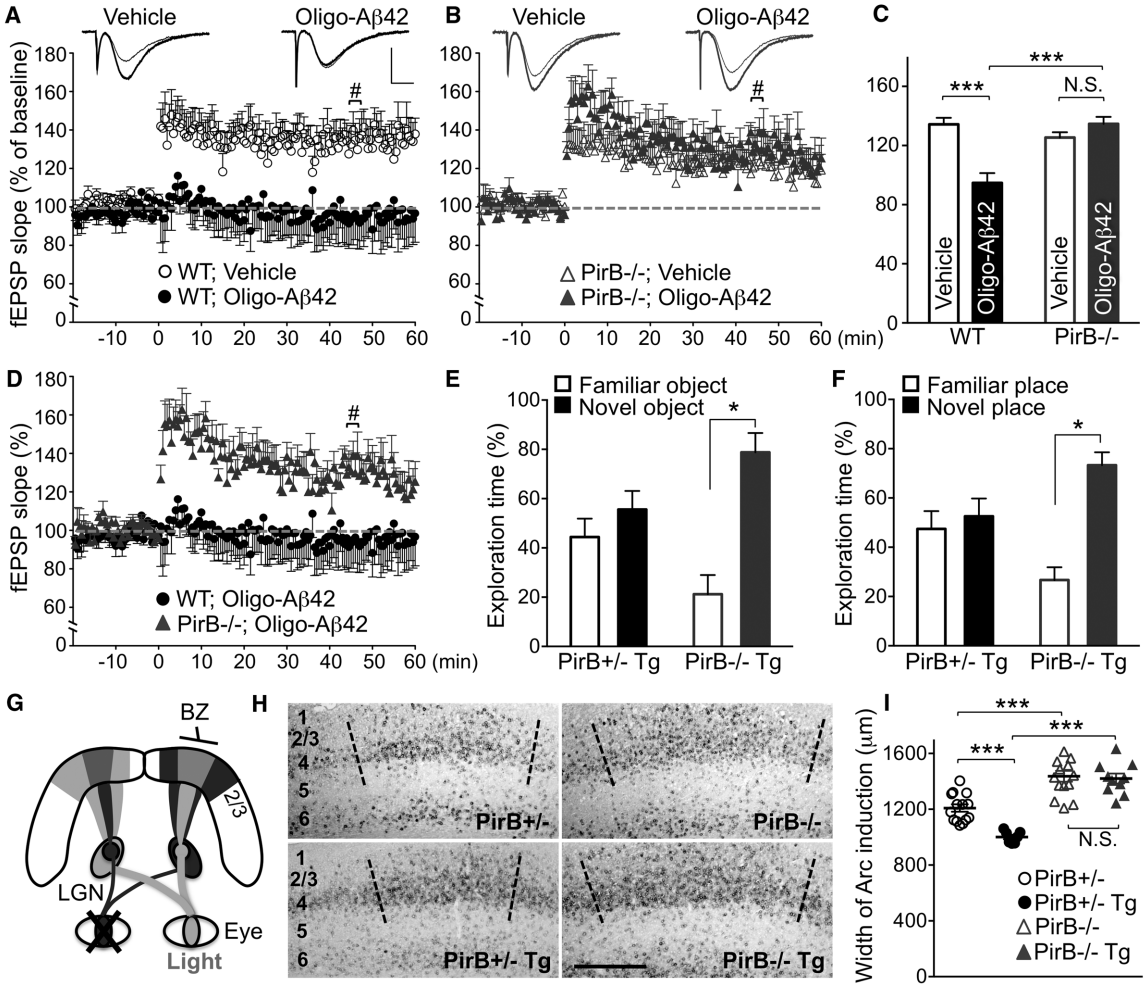

Fig. 3. PirB deletion rescues synaptic plasticity and behavioral deficits in AD models. (**A**) Acute application of oligo-Aβ42 inhibits LTP in WT hippocampal slices. fEPSPs were recorded from stratum radiatum in the CA1 region of hippocampal slices from 4- to 5-month-old WT mice with or without addition of oligo-Aβ42 (200 nM total peptide). Top panels show example fEPSP traces immediately before (light traces) and 45 min after (heavy traces) TBS; each is an average of five individual consecutive traces. Calibration bar = 0.5 mV/5 ms. The slope of the fEPSP after TBS, relative to baseline, is plotted as a function of time in the lower panel. Vehicle, n = 7 animals, 9 slices; Aβ42 oligomer, n = 6, 9 slices. (**B**) Aβ42 oligomer does not block LTP in PirB$^{-/-}$ slices. Vehicle, n = 5 animals, 8 slices; Aβ42 oligomer, n = 4, 6 slices. (**C**) Histograms of fEPSP slope measured 45 min after TBS. Each is a 2-min average of recordings taken from all slices of a given condition at time marked # in (A) and (B); all data are means ± SEM, ***P < 0.0001, t test. (**D**) Comparison of Aβ42 oligomer effects on hippocampal LTP from WT and PirB$^{-/-}$ mice; replotted from (A) and (B). (**E**) Novel object recognition memory of 9-month-old mice was evaluated by measuring percent of time mice spent exploring a novel versus a familiar object during a 10-min test session. (**F**) Novel place recognition memory (9-month-old) reflects percent time mice spent exploring familiar objects whose locations were or were not changed. Values are means ± SEM, *P < 0.05, paired t test. PirB$^{+/-}$; APP/PS1 (PirB$^{+/-}$ Tg, n = 6), PirB$^{-/-}$; APP/PS1 (PirB$^{-/-}$ Tg, n = 5). (**G**) Schematic of mouse visual system showing connections from eyes to lateral geniculate nucleus (LGN) to visual cortex. Cortical binocular zone (BZ) receives inputs from both eyes via the LGN. (**H**) In situ hybridization for Arc mRNA (digoxigenin-labeled antisense riboprobe) in visual cortex BZ of PirB;APP/PS1 littermates. At P22, one eye was removed; 10 days later (P32), induction of mRNA for the immediate early gene Arc at P32 was used to monitor width of territory receiving functional input from the open (ipsilateral) eye. Note that high Arc mRNA expression in layer 2/3 neurons within dashed lines, denoting domain of Arc induction in visual cortex. Scale bar, 500 μm. (**I**) Quantification of expansion in width of Arc mRNA signal in L2/3 visual cortex shown in (H). Data are means ± SEM; ***P < 0.001, t test; PirB$^{+/-}$ (n = 14 animals), PirB$^{+/-}$ Tg (n = 7), PirB$^{-/-}$ (n = 14), PirB$^{-/-}$ Tg (n = 10).

of layer 4 (fig. S7A) shares mechanisms with those that cause weakening of deprived-eye visually driven responses after monocular deprivation (*34*, *35*). The magnitude of LTD at L4 to L2/3 synapses in APP/PS1 mice is almost 3-fold greater than in nontransgenic littermates (fig. S7, B and C). This excessive LTD in PirB$^{+/-}$ Tg slices is not evident in PirB$^{-/-}$ Tg slices (fig. S7, B to D). Collectively, these data show that PirB function is associated not only with synaptic and cognitive alterations induced in adult mice by Aβ but also with loss of plasticity during early development in visual cortex of APP/PS1 mice.

Next, to identify signaling mechanisms engaged by the association of oligomeric Aβ with either PirB or LilrB2, we compared downstream signaling pathways in APP/PS1 mice with or without PirB. From an unbiased proteomic screen, we identified the actin-depolymerizing factor cofilin, as well as the serine-threonine phosphatases PP2A and PP2B/calcineurin, as potential PirB interactors. These candidates have already been implicated in Aβ-dependent synaptic loss and are engaged after induction of hippocampal LTD or LTP (*9*, *14*, *36*–*38*). In forebrains of APP/PS1 (PirB$^{+/-}$ Tg) mice, interactions of PirB with cofilin (Fig. 4A), as well as with protein phosphatases PP2A, B, or C (fig. S8), were increased relative to nontransgenic littermates. In contrast, other PirB signaling pathways, including tyrosine phosphorylation of PirB and its association with SHP-2 (*18*, *39*, *40*), were not significantly changed (Fig. 4A, lanes 1 and 2), nor were the levels of Aβ oligomers, including previously reported Aβ*56 (*41*) (56-kD high-*n* oligomers) (fig. S9; lanes 2 and 4). Together, these results suggest that the elevated interactions between PirB and cofilin or protein phosphatases in APP/PS1 mice are most likely to be caused by Aβ-PirB interactions.

PP2A and PP2B/calcineurin can activate cofilin by dephosphorylation at the Ser^3 residue (*42*, *43*), and the resulting actin filament disassembly appears to be crucial for Aβ oligomer–induced spine loss (*9*). Indeed, levels of cofilin phosphorylation at Ser^3 normalized to total cofilin levels were reduced about 40% in juvenile (P30) APP/PS1 forebrains (Fig. 4, B and D), as well as in adult (P200) hippocampal synaptosomes (Fig. 4, C and E), which were fully restored to normal levels by knocking out PirB (Fig. 4, B to E). Cofilin activity could be decreased by LIM kinase (LIMK) 1/2, an upstream kinase that phosphorylates cofilin at Ser^3; no evident change was detected in LIMK1/2 activity in APP/PS1 mice with or without PirB (Fig. 4, B to E), implying that PirB and LIMK signaling may regulate cofilin independently. Addition of Aβ42 oligomers to cultures of cortical neurons also consistently triggers cofilin activation (25% reduction in cofilin phosphorylation in wild-type neurons after 1 hour of treatment), as well as the loss of the postsynaptic protein PSD-95 (23% reduction after 24 hours of treatment) (Fig. 4, F and G). These changes did not occur in cortical neuron cultures from PirB$^{-/-}$ mice. Levels of cofilin phosphorylation in human Alzheimer's brains were reduced by about 38% relative to those in non-AD control brains (Fig. 4, H and I). In AD brains, elevated Tau phosphorylation was also observed (Fig. 4H), consistent with AD diagnosis (table S1). Thus, the PirB receptor may act directly to link Aβ-induced synaptotoxicity and cofilin or protein phosphatase pathways (*9*): Aβ oligomer–PirB binding would recruit cofilin-signaling modules to facilitate actin depolymerization, resulting in synaptic loss (indicated by reduction of PSD-95), ultimately leading to altered synaptic plasticity and cognitive deficits in APP/PS1

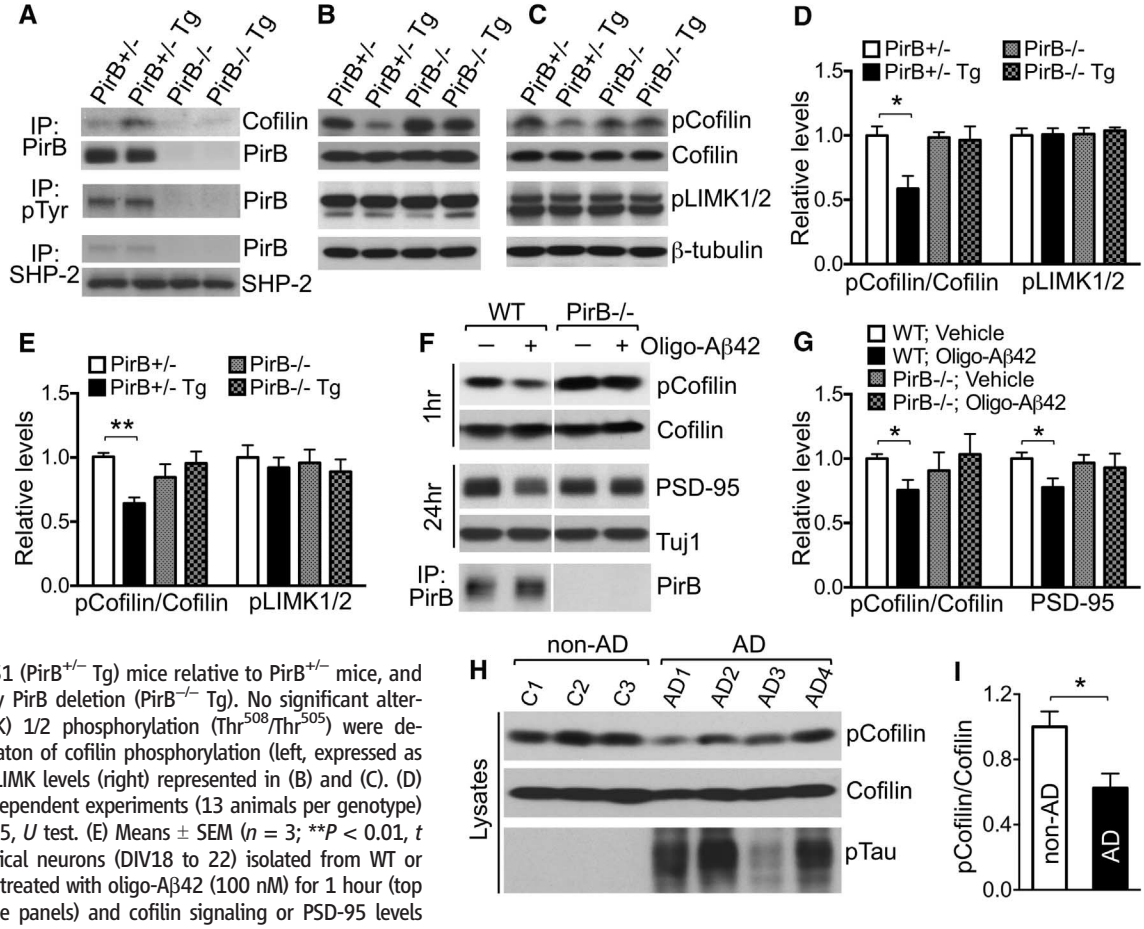

Fig. 4. Cofilin is recruited and activated by PirB in an Aβ-dependent manner in vivo and in vitro and is altered in human AD frontal cortex. (**A**) PirB interacts with cofilin in vivo in PirB$^{+/-}$ Tg mice (P30, forebrain), assessed by immunoprecipitation for PirB. Other known PirB-proximal signaling and interactions such as tyrosine phosphorylation of PirB and SHP-2 recruitment to PirB are not altered in PirB$^{+/-}$ relative to PirB$^{+/-}$ Tg mice. Representative data are shown ($n > 2$). (**B** and **C**) Cofilin phosphorylation is reduced in both (B) juvenile (P30, forebrain) and (C) adult (P200, hippocampal synaptosomes) PirB$^{+/-}$; APP/PS1 (PirB$^{+/-}$ Tg) mice relative to PirB$^{+/-}$ mice, and this reduction is rescued by PirB deletion (PirB$^{-/-}$ Tg). No significant alterations in LIM kinase (LIMK) 1/2 phosphorylation (Thr^{508}/Thr^{505}) were detected. (**D** and **E**) Quantificaton of cofilin phosphorylation (left, expressed as pCofilin/total cofilin) and pLIMK levels (right) represented in (B) and (C). (D) Means ± SEM from four independent experiments (13 animals per genotype) (*22*) shown in (B). *$P < 0.05$, *U* test. (E) Means ± SEM ($n = 3$; **$P < 0.01$, *t* test) shown in (C). (**F**) Cortical neurons (DIV18 to 22) isolated from WT or PirB$^{-/-}$ embryos (E16) were treated with oligo-Aβ42 (100 nM) for 1 hour (top panels) or 24 hours (middle panels) and cofilin signaling or PSD-95 levels were analyzed by Western blotting. Anti-Tuj1 (βIII-tubulin) antibodies detect neuronal tubulin. Bottom panels: Expression of PirB in these neurons detected by PirB immunoprecipitation. (**G**) Summary of cofilin phosphorylation (left; *$P < 0.05$, *U* test, $n = 7$) or PSD-95 levels (right; *$P < 0.05$, *U* test, $n = 6$) represented in (F). (**H**) Increased cofilin activity and Tau phosphorylation (Ser^{396}) in human frontal cortex specimens from Alzheimer's patients (AD1 to AD4) relative to non-AD adults (C1 to C3) (table S1), assessed by Western blot analysis. (**I**) Summary of cofilin phosphorylation cases represented in (H). Means ± SEM, *$P < 0.05$, *t* test.

mice (fig. S10). In the cerebral cortex of Alzheimer's patients, LilrB2 could engage similar cofilin-mediated downstream mechanisms.

Our results show that murine PirB and its human ortholog LilrB2 act as receptors for oligomeric forms of Aβ42. Mice lacking PirB are immune to the damaging effects of Aβ in hippocampal LTP and recognition memory, as well as to alterations in cofilin signaling and PSD-95 synaptic loss. We suggest that interactions between Aβ oligomers and PirB generate not only synaptotoxicity in mouse models of AD but also early defects in developmental plasticity present in visual cortex (*17*). The demonstration here that $PirB^{-/-}$ but not wild-type hippocampal slices are resistant to the acute effects of Aβ oligomers on LTP and that Aβ oligomers can alter cofilin signaling in wild-type but not $PirB^{-/-}$ cortical neurons in vitro, also argues that the rescue of AD phenotypes in $PirB^{-/-}$ Tg mice is via direct abrogation of PirB action, rather than indirect compensation or parallel signaling pathways. We also identify LilrB2 in human brain as an Aβ receptor that may contribute to synaptic loss and cognitive impairment in AD progression. Our results show that via PirB, Aβ oligomers can engage signaling pathways for neuronal actin organization that lead to synapse elimination. Therapies that selectively block LilrB2 function may be promising for treatment of AD even in the prodromal stage.

References and Notes

1. M. Sheng, B. L. Sabatini, T. C. Südhof, *Cold Spring Harb. Perspect. Biol.* **4**, a005777 (2012).
2. J. J. Palop, L. Mucke, *Nat. Neurosci.* **13**, 812–818 (2010).
3. M. Faizi *et al.*, *Brain Behav* **2**, 142–154 (2012).
4. C. Perez-Cruz *et al.*, *J. Neurosci.* **31**, 3926–3934 (2011).
5. S. Knafo *et al.*, *Cereb. Cortex* **19**, 586–592 (2009).
6. M. Cissé *et al.*, *Nature* **469**, 47–52 (2011).
7. F. Kamenetz *et al.*, *Neuron* **37**, 925–937 (2003).
8. J. Wu *et al.*, *Cell* **147**, 615–628 (2011).
9. G. M. Shankar *et al.*, *J. Neurosci.* **27**, 2866–2875 (2007).
10. G. M. Shankar *et al.*, *Nat. Med.* **14**, 837–842 (2008).
11. H. Hsieh *et al.*, *Neuron* **52**, 831–843 (2006).
12. J. Laurén, D. A. Gimbel, H. B. Nygaard, J. W. Gilbert, S. M. Strittmatter, *Nature* **457**, 1128–1132 (2009).
13. J. W. Um *et al.*, *Nat. Neurosci.* **15**, 1227–1235 (2012).
14. X. Wang *et al.*, *J. Alzheimers Dis.* **30**, 665–673 (2012).
15. J. L. Jankowsky *et al.*, *Hum. Mol. Genet.* **13**, 159–170 (2004).
16. M. Garcia-Alloza *et al.*, *Neurobiol. Dis.* **24**, 516–524 (2006).
17. C. M. William *et al.*, *J. Neurosci.* **32**, 8004–8011 (2012).
18. J. Syken, T. Grandpre, P. O. Kanold, C. J. Shatz, *Science* **313**, 1795–1800 (2006).
19. T. Takai, *Immunology* **115**, 433–440 (2005).
20. J. K. Atwal *et al.*, *Science* **322**, 967–970 (2008).
21. On the basis of size exclusion column chromatography (Fig. 1A) and Western blot analyses (Fig. 1B), as well as previous studies (*7*), the average degree of polymerization (DP) of oligomerized Aβ42 is estimated to be 60 (DPn ≈ 270 kD/4.5 kD). The mono-Aβ42 preparation consists almost exclusively of monomeric peptides with a small fraction (<5%) of low-*n* oligomers (dimer, trimer, or tetramer; Fig. 1, A and B).
22. See supplementary materials on *Science* Online.
23. H. D. VanGuilder Starkey *et al.*, *J. Mol. Neurosci.* **48**, 111–126 (2012).
24. K_d is calculated using concentration of monomer equivalent for total Aβ42 peptides (fig. S1A). Because the K_d of mono-Aβ42 is minimal (Fig. 1J), it is likely that the K_d for PirB and high-*n* Aβ42 oligomers is much lower than 180 nM. If the high-*n* species of Aβ42 responsible for binding have a DPn of ~60 (*21*) and consist of ~30% of total Aβ42 peptides (fig. S1A, and Fig. 1, A and B) (*22*), the corrected K_d would be ~1 nM.
25. T.-I. Kam *et al.*, *J. Clin. Invest.* **123**, 2791–2802 (2013).
26. J. Zheng *et al.*, *Nature* **485**, 656–660 (2012).
27. G. Ma *et al.*, *Immunity* **34**, 385–395 (2011).
28. The closest human homolog for murine PirB among the five members of the human leukocyte immunoglobulin (Ig)–like receptor B (LilrB) family has been considered to be LilrB3 based on overall amino acid sequence homology (Fig. 2A) (*27*). However, domain sequence analysis indicates that the D1D2 domain of LilrB2 aligns with the D1D2 domain of PirB, where Aβ oligomer binding occurs, whereas the D1D2 domain of LilrB3 aligns more closely with the D3D4 domain of PirB, which suggests that conservation present in the D1D2 domains, as well as tertiary structure surrounding Aβ binding site, is important for this binding.
29. M. Lindhagen-Persson, K. Brännström, M. Vestling, M. Steinitz, A. Olofsson, *PLoS ONE* **5**, e13928 (2010).
30. H. W. Kessels, L. N. Nguyen, S. Nabavi, R. Malinow, *Nature* **466**, E3–E4, discussion E4–E5 (2010).
31. S. J. Raiker *et al.*, *J. Neurosci.* **30**, 12432–12445 (2010).
32. P. L. McClean, V. Parthsarathy, E. Faivre, C. Hölscher, *J. Neurosci.* **31**, 6587–6594 (2011).
33. A. W. McGee, Y. Yang, Q. S. Fischer, N. W. Daw, S. M. Strittmatter, *Science* **309**, 2222–2226 (2005).
34. G. B. Smith, A. J. Heynen, M. F. Bear, *Philos. Trans. R. Soc. London Ser. B* **364**, 357–367 (2009).
35. R. A. Crozier, Y. Wang, C. H. Liu, M. F. Bear, *Proc. Natl. Acad. Sci. U.S.A.* **104**, 1383–1388 (2007).
36. S. Li *et al.*, *Neuron* **62**, 788–801 (2009).
37. H. Y. Wu *et al.*, *J. Neurosci.* **30**, 2636–2649 (2010).
38. M. B. Rust *et al.*, *EMBO J.* **29**, 1889–1902 (2010).
39. J. D. Adelson *et al.*, *Neuron* **73**, 1100–1107 (2012).
40. Y. Fujita, S. Endo, T. Takai, T. Yamashita, *EMBO J.* **30**, 1389–1401 (2011).
41. S. Lesné *et al.*, *Nature* **440**, 352–357 (2006).
42. P. J. Meberg, S. Ono, L. S. Minamide, M. Takahashi, J. R. Bamburg, *Cell Motil. Cytoskeleton* **39**, 172–190 (1998).
43. N. V. Oleinik, N. I. Krupenko, S. A. Krupenko, *Oncogene* **29**, 6233–6244 (2010).

Acknowledgments: We thank the Human Brain and Spinal Fluid Resource Center for providing human brain specimens; P. Kemper, C. Chechelski, and N. Sotelo-Kury for assistance with mouse husbandry; M. Stern for technical assistance; and C. Cepko (Harvard) for providing the pCAGIG vector. We also thank M. Frosch (MGH/Harvard) and M. Shamloo (Stanford Behavioral and Functional Neuroscience Laboratory, NIH grant NS069375) for helpful suggestions and advice. Supported by NIH grant EY02858 (C.J.S.), the G. Harold and Leila Y. Mathers Charitable Foundation (C.J.S.), the Ellison Medical Foundation (C.J.S.), NIH grant 5T32EY020485 (T.K.), a Regina Casper Stanford Graduate Fellowship (G.S.V.), NIH grant K08NS069811 (C.M.W.), NIH grant 5R01AG041507 (B.T.H.), an Alzheimer Disease Research Center pilot grant (NIH grant 5P50AG005134 to C.M.W.), NSF predoctoral fellowship (M.E.B.), and HHMI (K.C.G.). B.T.H. is on the Scientific Advisory Board of Neurophage and is a consultant and collaborator with Takeda Pharmaceutical Company, Bristol Meyer Squibb, Acumen, AZTherapeutics, Siemens, Sanofi, Neotope, and Fidelity Biosciences, none of which were involved in this study. C.J.S. and T.K. are inventors on a patent application assigned to the Board of Trustees of the Leland Stanford Junior University on methods and compositions for inhibiting the effects of β-amyloid oligomers (U.S. provisional application no. 61/777,835).

Supplementary Materials

www.sciencemag.org/content/341/6152/1399/suppl/DC1
Materials and Methods
Figs. S1 to S10
Table S1
References (*44*–*52*)

18 June 2013; accepted 29 July 2013
10.1126/science.1242077

An Epidermal MicroRNA Regulates Neuronal Migration Through Control of the Cellular Glycosylation State

Mikael Egebjerg Pedersen,[1] Goda Snieckute,[1] Konstantinos Kagias,[1] Camilla Nehammer,[1] Hinke A.B. Multhaupt,[2] John R. Couchman,[2] Roger Pocock[1]*

An appropriate balance in glycosylation of proteoglycans is crucial for their ability to regulate animal development. Here, we report that the *Caenorhabditis elegans* microRNA *mir-79*, an ortholog of mammalian *miR-9*, controls sugar-chain homeostasis by targeting two proteins in the proteoglycan biosynthetic pathway: a chondroitin synthase (SQV-5; squashed vulva-5) and a uridine 5′-diphosphate–sugar transporter (SQV-7). Loss of *mir-79* causes neurodevelopmental defects through SQV-5 and SQV-7 dysregulation in the epidermis. This results in a partial shutdown of heparan sulfate biosynthesis that impinges on a LON-2/glypican pathway and disrupts neuronal migration. Our results identify a regulatory axis controlled by a conserved microRNA that maintains proteoglycan homeostasis in cells.

Animal development requires the differentiation and assembly of distinct cell types into specific tissues and organs. During these processes, cells are guided by interactions with the extracellular matrix (ECM), which contains a variety of signaling molecules, including proteoglycans (*1*). Proteoglycans are made up of core proteins, such as syndecans, glypicans, and perlecans, that are decorated with varying numbers of long, unbranched glycosaminoglycan (GAG) chains. GAG chains vary in type and length and may be modified by sulfation and epimerization. Differential glycosylation and modification produce diverse interfaces for ligand-receptor interactions (*2*, *3*). These structural parameters must be regulated to permit the coordination of specific and context-dependent intercellular signaling events (*4*, *5*). The biosynthetic pathways that assemble and modify GAG chains on core proteins are highly conserved, and their disruption can cause developmental defects and lead to disease in many systems (*4*, *6*, *7*). GAG biosynthesis requires the transport of nucleotide sugars [uridine 5′-diphosphate

[1]Biotech Research and Innovation Centre, University of Copenhagen, Ole Maaløes Vej 5, Copenhagen, Denmark. [2]Department of Biomedical Sciences, University of Copenhagen, Denmark.
*Corresponding author. E-mail: roger.pocock@bric.ku.dk